

Excitation of ultrashort light pulses in a ruby ring laser with resonance loss modulation

G. V. Krivoshechekov, L. A. Kulevskii, N. G. Nikulin, V. M.

Semibalamut, V. A. Smirnov, and V. V. Smirnov

Semiconductor Physics Institute, Siberian Division, USSR Academy of Sciences;

P. N. Lebedev Physics Institute, USSR Academy of Sciences

(Submitted December 1, 1972)

Zh. Eksp. Teor. Fiz. **64**, 1997-2007 (June 1973)

The formation of ultrashort light pulses in a ruby ring laser with active resonance loss modulation is investigated experimentally and numerical calculations are performed by computer. It is shown that a stationary pulse is formed in the linear amplification range in such lasers and the laser parameters remain essentially constant in the non-linear range. As a result, lasers with active modulation can generate ultrashort pulses with stable parameters. The experimental results are in good agreement with the calculations. Ultrashort 10^{-10} sec pulses reproducible in successive flashes are obtained experimentally.

Ultrashort light pulses can be produced in lasers by some method of locking the axial modes of the resonator. The currently most widespread method of mode locking is self-locking in lasers with nonlinear absorbers^[1,2]. The general acceptance of this method is due to its technical simplicity and to the fact that nonlinear absorber lasers achieved record values of length and peak power of their ultrashort pulses. Nevertheless, as is shown in^[3-5], a regular sequence of single ultrashort pulses can be obtained from such lasers only with some probability. The time behavior of the emission is not always reproducible from flash to flash, because pulse shaping up to the bleaching of the nonlinear absorber is a random process^[3]. Poor reproducibility of the emission time behavior is a significant shortcoming of lasers with nonlinear absorbers.

There is another well known method of mode locking, i.e., the active modulation of laser parameters. The method is based on a resonant (at intermode frequency or its multiple) variation of the optical length (phase modulation)^[6,7] or a variation of resonator losses (amplitude modulation)^[8,9]. From now on we consider only the active loss modulation lasers. The modulators in such lasers are most often represented by acoustic^[8] or electro-optical^[10,11] shutters. In contrast to lasers with bleachable filters, such a modulation allows us to control the formation of ultrashort pulses and seems to offer in principle the possibility of obtaining pulses with good reproducibility of the parameters. The feasibility of generating stationary pulses in an active loss modulation laser was demonstrated, for example, in^[12,13]. However, that research failed to determine the stabilization time of the stationary pulse, which is an important characteristic of solid-state lasers operating in the pulsed mode. It is noted that stationary pulse stabilization time can be found only by investigating the pulse formation process in the laser. Such an investigation can also identify the amplification stage in which the stationary pulse was established. In^[12,13], this stage was determined for selected models, which are not applicable to lasers with Lorentz amplification line shape.

No investigator has examined whether stationary pulses can exist in lasers with Lorentz line shape, such as the ruby laser^[1], or the question of the effect of varying laser parameters on the stability of stationary pulses.

It is the above problems that are considered in this paper. The formation of ultrashort pulses in a ruby ring laser with resonance loss modulation is studied both by numerical computer simulation and by experimental methods. The simulation of laser operation is performed in the time domain, which is considered to be the more suitable approach. We calculated the pulse-parameter variation caused by the modulator and by the active medium after a complete pass. Multiple repetition of analogous computations allowed us to trace the entire process of ultrashort pulse formation in the laser. The computations show that the stationary pulse is established in the linear amplification stage. The stabilization time is determined by the effective gain of the laser and by the modulation law. The computation results are in good agreement with the results of experimental investigation of the ultrashort pulse-formation process.

NUMERICAL COMPUTATION

Computer simulation was performed for a ring resonator laser model with a one-dimensional active medium of length l ($0 \leq z \leq l$), representing an ensemble of two-level atoms with a homogeneously broadened line, and a loss modulator. All losses in the resonator were attributed to the modulator, whose effective transmission coefficient $\rho(t)$ was a time-periodic function with a period equal to the time of one round trip through the resonator.

The computation was commenced by specifying the initial noise field distribution from which the modulator shaped the initial (starting) pulse. The starting pulse was applied to the input ($z = 0$) of the active medium. The pulse generated by the starting pulse during the first trip was computed next. This pulse then served as the initial pulse for the second trip through the resonator. This computation was repeated for each of the subsequent trips.

In the computation it was assumed that the path of a pulse in the resonator can be divided into three sections: the active medium, free space, and the loss modulator. If we assume zero dispersion in free space, a change in the pulse can take place only in the active medium and in the modulator. Traversal of the free space in the resonator merely introduces a delay in the pulse.

The effect of the modulator is accounted for in a

simple manner, since modulator losses are independent of field intensity. The active medium thus represents the most complex section. The propagation of a light pulse in a two-level active medium with a homogeneously broadened line and with the pulse carrier frequency being in exact resonance with the atomic transition frequency ω_0 is described by equations for slowly varying amplitudes^[15-17]:

$$\frac{\partial E}{\partial z} + \frac{1}{c} \frac{\partial E}{\partial t} = \frac{2\pi\omega_0}{c} P, \quad (1)$$

$$\frac{\partial P}{\partial t} + \frac{1}{T_2} P = \frac{\mu^2}{\hbar} NE, \quad (2)$$

$$\frac{\partial N}{\partial t} + \frac{1}{T_1} (N - N_0) = -\frac{1}{\hbar} PE. \quad (3)$$

Here $E(t, z)$, $P(t, z)$, and $N(t, z)$ are slowly varying real amplitudes of the field, polarization, and population inversion; c is the speed of light; T_1 is the atomic longitudinal relaxation time; T_2 is the transverse relaxation time; N_0 is the initial population inversion; and μ is the matrix element of the dipole moment.

The factors that act in the linear and nonlinear amplification stages of the active medium are significantly different. In the linear amplification stage, the active-medium gain can be considered independent of field intensity. The determining factor in this stage is the frequency dependence of gain. This dependence is particularly effective if the linear amplification stage in the laser is long.

In a solid-state laser operating in the pulse mode, the pulse entering the linear stage removes the inversion rapidly (in a few trips). At the same time, to achieve a high emission power, we can shape the pulse in the linear amplification stage in a low-Q regime and then switch-on the full Q in the nonlinear stage. This further shortens the nonlinear amplification stage. The short duration of this stage leads us to assume that gain in this stage does not depend on frequency but only on field intensity.

The system (1)–(3) for the linear stage is easily solved by the Riemann method^[18], yielding

$$E(t', z) = E(t', z=0) + \int_0^{t'} E(t, z=0) \exp\left\{-\frac{(t'-t)}{T_2}\right\} \frac{I_1(2\sqrt{\alpha(t'-t)})\sqrt{\alpha z}}{\sqrt{t'-t}} dt. \quad (4)$$

Here $\alpha = 2\pi\mu^2\omega_0 N_0/c\hbar$; I_1 is a modified Bessel function of order 1; and $t' = t - z/c$. In the nonlinear amplification stage we consider only the case of noncoherent interaction of the pulse with the medium ($T_2 \ll \tau_p \ll T_1$, where τ_p is pulse length). The solution of (1)–(3) is known in this approximation^[19,20]:

$$I(t', z) = I(t', z=0) \left(1 - \left[1 - \exp\left\{-\sigma \int_0^{t'} N_0(t'=0, z') dz'\right\}\right] \times \exp\left\{-2\sigma c \int_0^{t'} I(t, z=0) dt\right\}\right)^{-1}, \quad (5)$$

$$N(t', z) = N_0(t'=0, z) \exp\left\{-\sigma \int_0^{t'} N_0(t'=0, z') dz'\right\} \times \left[\exp\left\{2\sigma c \int_0^{t'} I(t, z=0) dt\right\} + \exp\left\{-\sigma \int_0^{t'} N_0(t'=0, z') dz'\right\} - 1\right]^{-1}. \quad (6)$$

Here $\sigma = 4\pi\omega_0\mu^2 T_2/c\hbar$ is the transition cross section at the frequency ω_0 ; $I = cE^2/8\pi$ is the field intensity; and $t' = t - z/c$. We note that the expression

$$g(t') = \exp\left\{\sigma \int_0^{t'} N(t', z') dz'\right\}, \quad (7)$$

encountered in (5) and (6) is the gain of the active medium. In the computation, expression (4) was rewritten for intensity I .

The relationships (4) and (5) for $z=l$ connect the pulse shape at the output of the active medium ($I(t', z=l)$) with the input pulse shape ($I(t', z=0)$). At $t=T$ (T is the resonator round trip time) (6) determines the population inversion in the active medium ($N(t', z)$) after the pulse has passed through the value ($N_0(t'=0, z)$) of the inversion before the arrival of the pulse.

Equations (4)–(6) were the basis of the numerical simulation of the pulse propagation process in the active medium. The boundary conditions had the form

$$I_{k+1}(t)|_{z=0} = \rho(t) I_k(t), \quad (8)$$

where k is the number of round trips through the resonator and $I_k(t)$ is the pulse envelope after the k -th round trip, taking the corresponding delay into account.

The dependence of the gain of the active medium on field intensity in the resonator was constantly monitored in the computation of pulse evolution. The linear amplification stage lasted as long as the gain was independent of the intensity, and the computation was performed according to the corresponding formula (4). As soon as gain became dependent on intensity (varied by 1%), the nonlinear amplification stage began and the pulse evolution was computed according to (5) and (6).

The computation error was no worse than 0.1% per pass. The results of the computation are shown in Figs. 1–4.

Figure 1 shows the modulator transmission distribution in the period T ($T = 5 \times 10^{-9}$ sec is the round trip time through the resonator). It is described by the equation

$$\rho(t) = \rho_0 \cos^2 [0.3\pi \cos(2\pi t/T_M)] \quad (9)$$

(ρ_0 is the maximum transmission coefficient and T_M is the period of modulating voltage, $T_M = 2T$). The figure shows also the pulse envelopes after 1, 10, 50, 100, and 150 round trips in the linear amplification stage. Equation (9) corresponds to the transmission of an electro-optical modulator driven by sinusoidal voltage^[21]. It can be seen from Fig. 1 that at first the modulator “cuts out” a pulse from noise; the pulse maximum in the period T coincides with the loss minimum and the pulse length is determined by the modulator transmission law. The pulse length becomes progressively shortened by the modulator as the number of round trips through the resonator increases. At the same time, the pulse maximum becomes displaced to the right (delay). The pulse maximum continues shifting only up to a certain number of round trips (see the curve marked $k=150$), after which the maximum takes up a fixed position in the

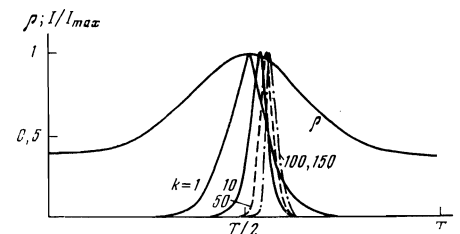


FIG. 1. Modulator transmission $\rho(t)$ per period and pulse envelope family for different round-trip numbers k .

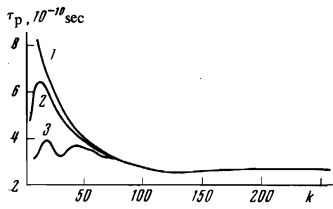


FIG. 2.

FIG. 2. Pulse length as a function of the number of resonator round trips for various initial field distributions: 1 - "smooth" initial field distribution; 2, 3 - intensity overshoots present in the modulation period T .

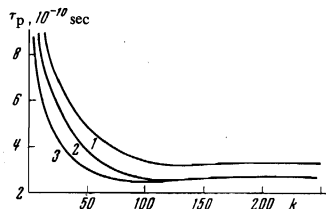


FIG. 3.

FIG. 3. Pulse length as a function of the number of resonator round trips for various loss modulation laws: 1 - $\rho(t) = \rho_0 \sin^2 [0.5\pi \sin(2\pi t/T_M)]$; 2 - $\rho(t) = \rho_0 \cos^2 [0.3\pi \cos(2\pi t/T_M)]$; 3 - $\rho(t) = \rho_0 \cos^2 [0.5\pi \cos(2\pi t/T_M)]^3$

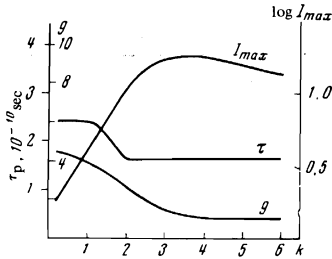


FIG. 4.

period. The length and shape of the pulse become stationary (lines for $k=100$ and 150) and the intensity increases in proportion to the number of round trips.

The reason why a stationary pulse occurs in the linear amplification stage becomes clear if we consider the simultaneous effect of modulator losses and the active medium gain on the pulse. Modulator losses shorten the pulse during each successive round trip, so that an ever shorter pulse travels through the active medium. Now, we know the effect of the active medium on pulses of different length [22]. As the entering pulse length τ_p shortens, the gain of the active medium decreases, the pulse lengthens, and the lag of the pulse peak increases because the group velocity of the pulse decreases in the active medium. However, as long as $\tau_p \gg T_2$, the pulse does not broaden significantly in the active medium, and only the pulse maximum is delayed. Significant pulse broadening is observed if pulse length τ_p is comparable with T_2 .

Consequently, the initial traversals ($\tau_p \gg T_2$) result in pulse shortening due to the modulator, while the active medium merely delays the pulse maximum. This pulse shortening continues until the pulse length becomes comparable with T_2 (in order of magnitude). As soon as comparability is reached, the pulse begins to broaden. Thus we observe a situation in which the shortening of the pulse per pass, effected by the modulator, is compensated by pulse broadening during the same pass through the active medium. In this case the pulse length and its position in the period do not change during the subsequent trips in the resonator. The pulse becomes stationary. The shape of the stationary pulse is determined by the modulation law.

We note that the stabilization of the stationary pulse occurs in the linear amplification stage after a large number (~ 500) of trips. In order for the pulse to remain in this stage for such a long time, the effective gain²⁾ must be small (~ 1.05 for a maximum modulator trans-

mission). When the effective gain is large, field intensity quickly reaches saturation and the nonlinear amplification stage begins before the pulse can become stationary.

Figure 2 shows the pulse length τ_p at half width in the linear amplification stage as a function of the number of round trips through the resonator, for one type of modulation law (9) and for various initial field distributions. We see that the length of a stationary pulse does not depend on the initial field distribution. The difference in length appears only in the early formative stage of the stationary pulse. In this stage the pulse parameters are determined to a considerable extent by the initial field distribution. It follows from Fig. 2 that pulse parameters with fixed linear development time are not reproducible at large effective gains, when stationary pulse cannot establish itself in the linear amplification stage.

Figure 3 shows the pulse length τ_p as a function of the number of round trips k for one shape of the starting wave (one initial field distribution) and various modulation laws. Figure 3 illustrates the fact that an increasing slope of the modulating function (see lines 1, 2, and 3, which are arranged in the order of increasing slope of the function $\rho(t)$) weakly affects the length of the stationary pulse. The increasing slope of the function $\rho(t)$ increases the pulse compression rate.

Figure 4 pertains to the nonlinear pulse amplification stage. The diagram shows the gain g (see (7)), the logarithm of relative peak intensity ($\log I_{max} = \log(I_k \max / I_0 \max)$), and the pulse length τ_p at half-width as functions of the number k of round trips through the resonator. It is apparent that the gain of the active medium decreases in the nonlinear stage (saturation effect). Pulse intensity decreases exponentially. We also observe a slight shortening of the pulse caused by the preferential amplification of the pulse front.

EXPERIMENTAL RESULTS

The formation of ultrashort pulses was investigated experimentally with the setup shown in Fig. 5. The laser resonator (optical length of 150 cm) formed a ring based on four dispersionless prisms P . The active material K was a 5.5×120 mm ruby crystal. There was no axial mode selection. Diaphragms D , 1.8 mm in diameter, eliminated the transverse modes.

Resonance loss modulation was obtained by an electro-optical method using the LiNbO_3 crystal M_2 . A half-wave phase shift for LiNbO_3 at $\lambda = 0.7 \mu$ required 580 v.

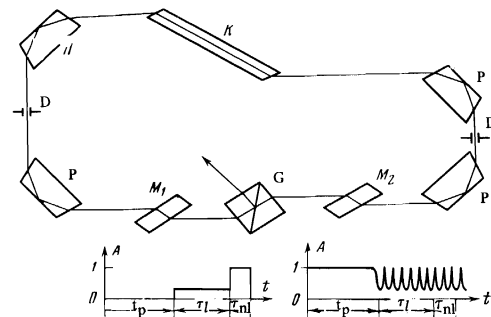


FIG. 5. Experimental setup: K - crystal; P - nondispersion prisms; D - iris; M_1, M_2 - modulators; G - Glan prism. Bottom: nomograms illustrating the transmission of electro-optical modulators: t_p - pumping time; τ_l - linear amplification time; τ_{nl} - nonlinear amplification time.

Modulator M_1 (KDP crystal) served as the Q-switch in the nonlinear amplification stage and as a radiation outlet from the resonator. The nomograms in Fig. 5 illustrate the operation of the system. First the minimum-Q voltage is applied to switch M_1 . At the point of maximum inversion M_1 partially switches-in the cavity Q. A sinusoidal voltage, whose half period $T_M/2 = 5$ nsec equals the pulse round trip time, is simultaneously applied to M_2 . After the time τ_l corresponding to the linear development of generation, M_1 turns on the full Q. In the course of several round trips at high g_{eff} the pulse intensity increases sharply and a high-power pulse appears in the resonator. The pulse power continues to increase during the subsequent round trips while the medium gain decreases (nonlinear amplification process). When the pulse reaches maximum power ($g \approx 1$), switch M_1 turns on the Q and the pulse is let out of the resonator through a Glan prism. Since the backward wave was not suppressed, two pulses moving in opposite directions were formed simultaneously. However the pulses did not encounter each other in the active medium because of the appropriate placement of the loss modulator relative to the ruby crystal.

The experimental investigation was divided into two parts. In the first part we studied the effect of the linear development time on the following parameters: length, shape, and spectrum of the emitted pulse. A photoelectron recorder with a resolution of 10^{-11} sec was used to observe the length and shape of the pulse. The spectrum of the emitted pulse was recorded with a spectrograph (dispersion of 7.5 \AA/mm) with a resolution of 0.09 cm^{-1} . The linear development time was controlled by varying the transmission of modulator M_1 in the linear amplification stage. Modulator M_2 provided a 70% depth of modulation which remained constant during the experiment. In order to limit the observation to the linear amplification stage, the pulse was let out of the resonator for each τ_l at a point when its energy was low and just adequate to activate the measuring instruments.

Figure 6 shows intensity diagrams of pulses and the corresponding spectra for various values of the linear development time. When the linear development time is short, the laser generates relatively long pulses; the pulses and the corresponding spectra have a complex shape that is not reproducible from flash to flash (Fig. 6 a and b). The emitted pulses have a "pedestal" (non-locked modes) and an approximate estimate of the degree of mode-locking yields $\tau_p \Delta\nu = 20-50$. As τ_l increases, the pulse shortens and its shape and spectrum acquire more regularity (Fig. 6 c). For $\tau_l \geq 1.7 \text{ \mu sec}$, the shape of the pulses becomes simple and the spectrum is smooth [23]. The pulse length ($\tau_p \approx 10^{-10}$ sec) and spec-

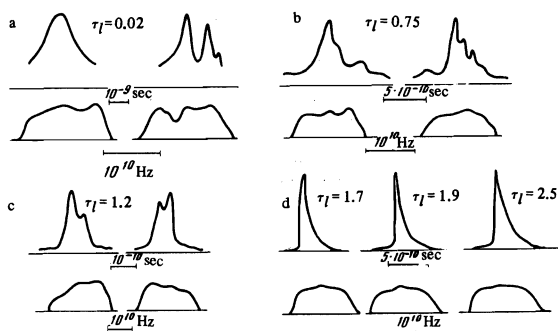


FIG. 6. Intensity diagrams for pulses and the corresponding spectra for various τ_l (in μsec).

tral width become stabilized and $\tau_p \Delta\nu \sim 3$. Figure 6 d shows intensity diagrams of pulses and spectra averaged for 15 flashes. An increase of the linear development time to 2.5 \mu sec caused no changes (within the limits of experimental accuracy) in the pulse parameters.

Figure 7 shows the pulse length τ_p as a function of the linear development time τ_l . Line 1 represents a theoretical function for an initial field distribution of the $E(t) = E_0$ type and the modulation law $\rho(t)$ used in the experiment. We see that the theoretical curve is in a good agreement with the experiment in the region of long linear development time. For short τ_l the experimental function $\tau_p(\tau_l)$ is represented by a broad band that shortens with increasing τ_l . This confirms the theoretical conclusion that the pulse has not enough time to assume the stationary form within a short linear amplification stage. Therefore for equal τ_l successive flashes generate pulses whose length varies within the band shown in the diagram.

We note that line 2 contains points of maximum possible pulse length for fixed τ_l . Such long pulses are obtained in the case of a "smooth" initial field distribution, i.e., when there are no intense excursions in the period of modulation. Indeed, in such a case, the modulator first "carves out" the pulse from the noise field, the pulse shape being determined by the modulation law. The pulse length then shortens in the linear amplification stage down to a value determined by the duration of the stage. Thus we see that in Fig. 7 line 2 coincides with the theoretical line 1 in the region of short τ_l for the case of a "smooth" initial field distribution.

In the second part of the experiment we studied the pulse behavior in the nonlinear amplification stage.

According to calculations, the power of the generated pulse is maximum at the point of saturation of the gain (See Fig. 4), i.e., after the pulse has passed the nonlinear amplification stage. In order to observe the evolution of pulse parameters in the course of the nonlinear amplification process, the pulse was allowed to leave the laser after different time intervals from the point of total Q. We recorded the same pulse parameters as in the first part of the experiment: shape, length, and spectrum. The parameters of 15 pulses were recorded for each time interval. The results of measurements showed that nonlinear amplification causes merely a slight (~ 1.5 times) shortening of the pulse front with the other pulse parameters (within experimental accuracy) remaining unchanged.

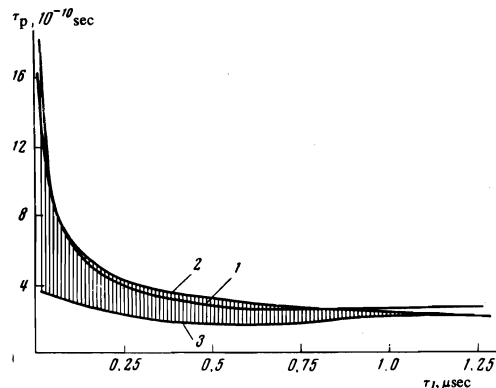


FIG. 7. Pulse length as a function of linear development time; line 1 — theoretical; lines 2 and 3 limit the region of experimental data.

The single ultrashort pulses obtained in the experiment had a maximum power of ~ 8 MW and a divergence close to the diffraction limit.

CONCLUSION

The calculations and experimental investigation of a ruby ring laser with resonance loss modulation prove the feasibility of generating ultrashort pulses with adequate stability in such a laser.

The stability of ultrashort pulses is due to the fact that a stationary pulse is established in the laser in the linear amplification stage and that pulse parameters do not change significantly in the nonlinear amplification stage. The pulse becomes stationary by virtue of the joint action of two factors: compression due to modulation and expansion in the active medium. The establishment of the stationary form of the ultrashort pulse requires a long time ($\sim 2 \times 10^{-6}$ sec). To obtain such a long stage of linear amplification, we must ensure a low effective gain. The reduced effective gain imparts low power to the emitted pulses because of the decreased amplification in the active medium. A higher power of ultrashort pulses can be obtained by Q-switching, so that for a high effective gain of the active medium pulses are formed in the linear amplification stage at low Q (large losses) and the Q is turned on fully in the nonlinear amplification stage. Ultrashort pulses formed by the method of resonance loss variation in the ruby laser are relatively long ($\sim 10^{-10}$ sec). However, using such a laser as a driving generator, we can obtain shorter and yet powerful ultrashort pulses with stable parameters by means of cascade amplification. The stability of pulse parameters from flash to flash, the comparative simplicity of generating either single ultrashort pulses or series of pulses (with a controllable number of pulses in a series), and the controlled timing of an ultrashort pulse with an accuracy of $\sim 10^{-9}$ sec render such a laser a valuable and useful instrument for scientific research.

The authors thank A. M. Prokhorov for support in this work and Yu. N. Polivanov for useful discussion.

¹⁾Except for [14], which is mainly concerned with hysteresis phenomena in active loss-modulation laser.

²⁾The effective gain of a laser if $g_{\text{eff}}(t) = \rho(t)g(t)$.

- ¹A. J. DeMaria, W. H. Glenn, Jr., M. J. Brienza, and M. E. Mack, Proc. IEEE 57, 2 (1969).
- ²P. W. Smith, Proc. IEEE 58, 1342 (1970).
- ³B. Ya. Zel'dovich and T. I. Kuznetsova, Usp. Fiz. Nauk 106, 47 (1972) [Sov. Phys.-Usp. 15, 25 (1972)].
- ⁴V. S. Letokhov, Zh. Eksp. Teor. Fiz. 55, 1077, 1943 (1968) [Sov. Phys. JETP 28, 562, 1026 (1969)].
- ⁵T. I. Kuznetsova, Zh. Eksp. Teor. Fiz. 57, 1673 (1969) [Sov. Phys. JETP 30, 904 (1970)].
- ⁶A. Yariv, J. Appl. Phys. 36, 388 (1965).
- ⁷S. E. Harris and R. Targ, Appl. Phys. Lett. 5, 202 (1964); S. E. Harris and O. P. Duff, IEEE J. Quant. Electron. QE-1, 245 (1965).
- ⁸L. E. Hargrove, R. L. Fork, and M. A. Pollack, Appl. Phys. Lett. 5, 4 (1964).
- ⁹M. DiDomenico, J. Appl. Phys. 35, 2870 (1964).
- ¹⁰A. J. DeMaria and D. A. Stetser, Appl. Phys. Lett. 7, 71 (1965).
- ¹¹L. M. Osterink and J. D. Foster, J. Appl. Phys. 39, 4163 (1968).
- ¹²V. I. Bespalov and E. Ya. Daume, Zh. Eksp. Teor. Fiz. 55, 1321 (1968) [Sov. Phys. JETP 28, 692 (1969)].
- ¹³D. J. Kuizenga and A. E. Sogman, IEEE J. Quant. Electron. QE-6, 694 (1970).
- ¹⁴Y. Cho and H. Geffers, Opt. Communic. 4, 29 (1971).
- ¹⁵P. G. Kryukov and V. S. Letokhov, Usp. Fiz. Nauk 99, 169 (1969) [Sov. Phys.-Usp. 12, 641 (1970)].
- ¹⁶A. I. Isevgi and W. E. Lamb, Jr., Phys. Rev. 185, 517 (1969).
- ¹⁷G. L. Lamb, Jr., Rev. Mod. Phys. 43, 99 (1971).
- ¹⁸R. Courant and D. Hilber, Methods of Mathematical Physics, Wiley, 1953.
- ¹⁹L. M. Frantz and J. S. Nodvik, Appl. Phys. 34, 2346 (1963).
- ²⁰T. M. Il'inova and R. V. Khokhlov, Radiofizika 8, 899 (1965).
- ²¹E. R. Mustel' and V. N. Parygin, Metody modulyatsii i skanirovaniya sveta (Methods of Modulation and Scanning of Light), Nauka, 1970.
- ²²V. G. Savel'ev, Radiotekh. i elektron. 12, 361 (1967).
- ²³V. I. Malyshev, A. V. Masalov, and A. A. Sychev, Zh. Eksp. Teor. Fiz. 59, 48 (1970) [Sov. Phys.-JETP 32, 27 (1971)].

Translated by S. Kassel
214